BJET
(Bayero Journal of Engineering and Technology)
https://bjet.ng/index.php/jet

Research Article
2025, Vol. 20 (2), 5-14

VALORIZATION OF WASTE SODA LIME SILICA GLASS FOR THE FABRICATION OF ZnO/SLS GLASS SYSTEM: THERMAL AND COMPOSITIONAL ANALYSIS FOR ADVANCED MATERIAL APPLICATIONS

I. M. Alibe [1, *], S. Nasir [2], M. H. Mohd Zaid [3*], A. M. Alibe [4]

[1]Mechanical Engineering, Nigerian Army University Biu. PMB 1500, Biu, Borno State, Nigeria

[2] *Department of Chemistry, Federal University Dutse, P.M.B. 7156, Dutse, Jigawa State, Nigeria*

[3] Department of Physics, Universiti Putra Malaysia, 43400 UPM Serdang, Selangor, Malaysia

[4] *Mechanical Engineering Department, Federal Polytechnic Damaturu, P.M.B. 1006, Damaturu, Yobe State, Nigeria*

[*]Email: babaiya1@gmail.com; mhmzaid@upm.edu.my

Received: 17-05-2025
Accepted: 01-07-2025
Revised: 23-07-2025
Published: 13-08-2025

Abstract: *The increasing demand for sustainable materials in advanced technologies has driven significant research into the valorization of industrial and post-consumer waste, with soda lime silica (SLS) glass emerging as a viable precursor for low-energy optoelectronic applications. This study presents a comprehensive investigation into the thermal, compositional, physical, structural, and optical characteristics of a novel ZnO/SLS glass system synthesized via the conventional melt-quenching technique. Energy Dispersive X-ray Fluorescence (EDXRF) analysis confirmed that the primary oxide components ZnO, SiO_2, CaO, and Na_2O comprised approximately 95 wt.% of the total composition, while minor and trace oxides such as K_2O, MgO, BaO, Cr_2O_3, Fe_2O_3, and B_2O_3 were present in lower concentrations. Increasing ZnO content led to a proportional reduction in the concentration of other major oxides, resulting in optimized compositional tuning that enhanced the physical properties and chemical durability of the glass. Differential Thermal Analysis (DTA) revealed a progressive decrease in both the glass transition temperature (Tg) and crystallization temperature (Tc) with rising ZnO levels, attributed to reduced melt viscosity. Correspondingly, the glass density increased from 2.520 to 2.842 g/cm³, primarily due to the higher atomic mass of Zn and associated modifications in the glass network's cross-linking density. X-ray diffraction (XRD) patterns confirmed the amorphous nature of all samples through the presence of broad halos within the 2θ range of 20°–40°, with the observed shift toward higher angles and halo narrowing indicating reduced interatomic spacing due to Zn^{2+} substitution for larger Na^{+} and Ca^{2+} ions. Field Emission Scanning Electron Microscopy (FESEM) further corroborated the amorphous structure, revealing smooth, featureless surfaces devoid of crystallization, and indicating that ZnO incorporation does not induce microstructural disruption within the investigated composition range. These findings underscore the potential of ZnO/SLS glass systems as sustainable candidates for next-generation optoelectronic and functional glass applications.*

Key words: Thermal analysis; EDXRF; Density; Melt-quenching; Waste SLS glass.

1 Introduction

Reducing waste and CO_2 emissions, conserving energy and raw materials, and protecting the environment have become critical imperatives in modern society. Recycling, therefore, is essential for ensuring a sustainable future on this planet, and communities worldwide are increasingly encouraged to participate in the recycling loop (Liu et al., 2024; Singh et al., 2025). Although glass recycling has been practiced from ancient times (Baek et al., 2025; Kua et al., 2024), and glass containers were reused regularly in the nineteenth and twentieth centuries, present-day large-scale recycling started only in the 1970s (Dyer, 2014). The switch from the debatably more sustainable and environmentally conscious reuse to the more "convenient" recycling occurred through the promotion of technological advancements and marketing (Baek et al., 2025). This transition could historically be interpreted as a downgrade caused by a shift in consumption dynamics, symptomatic of our "throwaway culture" (Franjić and Freestone, 2018) , However, the aftermath of the switch is that nowadays glass is recycled almost everywhere across the globe, to varying extents (Del Rio et al., 2022).

In recent times, the management of solid waste has emerged as a critical challenge within the industrial sector (Lakhouit et al., 2025; Waite, 2025). A significant proportion of these wastes are disposed of in landfills; however, many nations face constraints due to the limited availability of appropriate landfill sites (Kubanza, 2025; Rashid et al., 2025). Moreover, this disposal approach is recognized as environmentally unsustainable (Kubanza 2025). To address this issue, numerous strategies involving the treatment and recycling of solid waste have been developed, aiming to mitigate the adverse environmental impacts (Kubanza, 2025; Rashid et al., 2025). Among the various waste materials suitable for recycling, soda lime silica glass stands out as a widely recovered resource with the potential for conversion into value-added products (Ezra et al., 2024). For effective recycling, waste glass must be sorted according to chemical composition and color, as recycled glass retains its original hue (Ismaeel et al., 2023). Consequently, glass recyclers often collect colourless, green, and brown (amber) glass separately these being the most prevalent types used in consumer packaging (Imteaz et al., 2012, 2021). Incorporating recycled glass into manufacturing processes offers several benefits, including conservation of natural resources, reduction in energy usage, and minimization of landfill volume (Rashid et al., 2025). The application of waste glass as a raw material in the synthesis of glass-ceramic products has gained significant interest, prompting extensive research in this domain.

Among commercially available glass types, soda lime silica (SLS) glass represents the most extensively manufactured and utilized category, accounting for approximately 90–95% of global glass production (Sinton and LaCourse, 2001). This predominance is largely attributed to its favourable glass-forming characteristics, which surpass those of many other conventional glass systems (Abbasi and Hashemi, 2014). Due to its versatility and desirable physical properties, SLS glass is widely employed in various applications, including window glazing, container manufacturing, flat glass production, packaging, thermal insulation, biomedical components, and construction materials (Francis et al., 2004; Franjić and Freestone, 2018; Chima, 2023; Ezra et al., 2024). The fabrication of precursor glass and its subsequent transformation into glass-ceramic materials generally involves two primary approaches: the melt-quenching technique and controlled heat treatment. Initially, raw materials with a specific compositional formulation are melted in a crucible or furnace at temperatures ranging from 1000 °C to 1600 °C, depending on the glass chemistry (Mohd Shofri et al., 2020). In the melt-quenching method, the molten material is rapidly cooled and formed into a bulk glass product using conventional shaping techniques (Samsudin et al., 2015). For powder-based processing, the molten glass is quenched in water to form glass frits, which are then ground into fine powder (Zaid et al., 2016). This powder is subsequently compacted through a palletizing process. The transformation of precursor glass into glass-ceramic occurs through controlled crystallization, where the avoidance of spontaneous devitrification during initial glass formation is critical (Zaid et al., 2016). Achieving optimal glass-ceramic properties requires the development of a high density of nucleation sites within the glass matrix, which is typically accomplished through a two-stage heat-treatment cycle: the first step promotes nucleation at a lower temperature, followed by a higher-temperature phase that supports crystal growth (Zaid et al., 2016; Abdel-Hameed et al., 2024; Almendro-Candel and Jordán Vidal, 2024). Thermal treatment plays a pivotal role in modifying the structural characteristics of glass-ceramics (Almendro-Candel and Jordán Vidal, 2024; Ezra et al., 2024). The application of thermal energy during this process densifies the material and increases the average grain size, enhancing its mechanical properties (Mohd Shofri et al., 2020). Heat treatment is widely utilized in powder metallurgy and ceramics manufacturing due to its effectiveness in transforming porous, compacted powder into mechanically robust bodies. This thermal processing influences key properties, including

hardness, grain morphology, crystal structure, and strength (Dang et al., 2017; Li et al., 2025; Samsudin et al., 2015; Tulyaganov et al., 2025). Notably, heat treatment enables the formation of materials with uniform porosity and near-net shapes unattainable through alternative techniques. It also facilitates the development of nano- or microcrystalline ceramic phases with superior performance relative to their amorphous precursors. The heating protocol must be carefully controlled typically within 2 at 10 °C/min to prevent internal stresses, with nucleation conducted at specific temperatures for 0.5 to 2 hours, followed by exposure to growth temperatures to promote crystallization (Zhang et al., 2010; Almendro-Candel and Jordán Vidal, 2024). Ultimately, the heat treatment profile determines the resulting material's crystallinity and phase composition, which directly impacts thermal expansion behavior, microstructure evolution, and the overall performance of the final glass-ceramic product (Samsudin et al., 2015; Zaid et al., 2016; Dang et al., 2017).

2 Experimental

2.1 Materials Preparation

The waste SLS glass bottle was chosen from the same brand of life ketchup produced by Life Group SDN. Bhd., and taken from recycling containers located at pizza hut restaurant, Mines Resort City, Serdang, Selangor, Malaysia. After being cleanly washed, the waste glass bottles are crushed to small pieces of glass cullet using stainless steel plunger and then finely ground using mortar and pestle to obtain the fine powder. After that, by using a specific size sieve, the fine powder is sieved obtain the powder of size ≤ 63 µm. Analytical-grade ZnO powders was procured from Sigma-Aldrich and used as received, without further purification. A series of precursor glass are prepared by mixing together a high purity raw materials such as ZnO (99.99%, Aldrich) and waste SLS glass powder referring to the empirical formula x(ZnO)100-x(SLS) where x = 0, 10, 20, 30, 40 and 50 wt.%. Figure 1. illustrate the schematic representation of the mechanism involved in the production of the glass-ceramics. The values of chemical composition based on the empirical formula are shown in the Table 1.

Table 1: Chemical composition of ZnO-SLS based glass.

Empirical Formula	Weight (g)		
	ZnO	**SLS**	**ZnO-SLS**
(SLS)	0.00	50.00	50.00
10(ZnO)90(SLS)	5.00	45.00	50.00
20(ZnO)80(SLS)	10.00	40.00	50.00
30(ZnO)70(SLS)	15.00	35.00	50.00
40(ZnO)60(SLS)	20.00	30.00	50.00
50(ZnO)50(SLS)	25.00	25.00	50.00

The conventional melt-quenching technique used in this studremains one of the most established and widely adopted methods for fabricating glassy materials, primarily due to its effectiveness in producing a broad spectrum of oxide-based glasses (Dang et al., 2017; Tulyaganov et al., 2025). This process involves the rapid cooling of a molten compound to prevent the nucleation and growth of crystalline phases, thereby preserving the amorphous structure of the material (Del Rio et al., 2022; Madival and Rajiv, 2025). The cooling rate must be sufficiently high to inhibit crystallization, ensuring the formation of a homogeneous glass matrix (Zaid et al 2016).

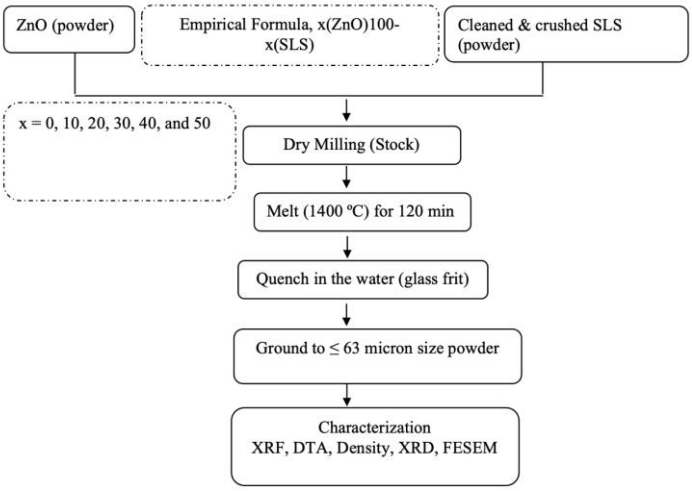

Figure 1: *Schematic representation of the mechanism involved in the production of glass-ceramics.*

Prior to initiating the melting process, it is critical to determine the appropriate glass melting temperature, as this varies significantly depending on the oxide composition of the raw materials. For instance, SLS

glass typically melts at approximately 900 °C, whereas ZnO requires a much higher melting point, around 1600 °C. In the present study, a mixture of SLS and ZnO-based oxides was melted at a selected temperature of 1400 °C for a duration of two hours. Approximately 50 g of the homogenized batch was transferred to an alumina crucible and subjected to thermal processing in an electric furnace under the specified conditions. Upon complete melting, the viscous melt was rapidly quenched in deionized water to form transparent glass frits, which were subsequently used for further processing (Zaid et al 2016; Ezra et al., 2024).

2.2 Characterization

In this study, a combination of analytical techniques; Energy Dispersive X-ray Fluorescence (EDXRF), Differential Thermal Analysis (DTA), X-ray Diffraction (XRD), and Field Emission Scanning Electron Microscopy (FESEM)—was employed to comprehensively characterize the elemental composition, thermal behavior, phase structure, and microstructure of glass and glass-ceramic samples. EDXRF analysis, a non-destructive method for qualitative and quantitative elemental determination (Yao et al., 2015), was performed on powdered samples using EDX-720, EDX-800HS, and EDX-900HS spectrometers, which feature integrated X-ray sources and solid-state detectors. The powders were loaded onto standardized holders, automatically transferred to the measurement chamber, and irradiated with high-energy X-rays, inducing the emission of characteristic fluorescent X-rays that were captured and processed in real time to determine the elemental composition. DTA was conducted to assess thermal properties such as glass transition, crystallization, and melting behaviors of the glass powders (45–100 µm) using a Diamond Pyris TG/DTA system (Perkin Elmer). The measurements were performed under a dynamic nitrogen atmosphere (flow rate: 50 cm^3/min) over a temperature range of 400 °C to 900 °C, using alumina (Al_2O_3) as the inert reference and a controlled heating rate of 10 °C/min to ensure accurate thermal event detection. XRD analysis was employed to identify the amorphous and crystalline phases using a PANalytical (Philips PW3040/60) diffractometer equipped with a CuKα radiation source operating at 40 kV and 30 mA. Diffraction data were collected over a 2θ range of 20° to 80°, and phase identification was performed by comparing experimental patterns with standard reference data using proprietary software, ensuring precise structural determination. Finally, FESEM analysis was conducted using a high-resolution FEI NOVA NanoSEM 230 to investigate the surface morphology and microstructural evolution of both untreated and heat-treated samples. Prior to imaging, samples were coated with a 50–70 Å thick gold layer via spin coating to prevent charging effects during electron beam exposure. The coated samples were mounted on stubs and introduced into the high-vacuum chamber, where they were analyzed at high magnification. Micrographs provided detailed surface topography, and grain size measurements were performed using the linear intercept method to assess microstructural uniformity, which is critical for evaluating material performance and processing efficiency.

3 Results and Discussion

3.1 EDXRF Analysis

The elemental composition of each precursor glass was determined through Energy Dispersive X-ray Fluorescence (EDXRF) spectroscopy, a non-destructive and reliable analytical technique for quantifying elemental concentrations in solid materials (Yao et al., 2015). The EDXRF analysis results are presented in Table 2, with all values reported in their oxide form to reflect the glass network's chemical structure. As illustrated in Figures 2 through 7, the predominant oxides identified in the precursor glass samples include ZnO, SiO_2, CaO, and Na_2O, collectively comprising approximately 95 wt.% of the total glass composition. These oxides play a critical role in defining the physical and chemical properties of the resulting glass-ceramic system (Zaid et al., 2016). Other constituents, such as K_2O and MgO, occur in smaller quantities and serve as modifiers or stabilizers within the matrix. Additionally, trace elements such as BaO, Cr_2O_3, Fe_2O_3, and B_2O_3 are present at concentrations generally below 1 wt.%, suggesting minimal influence on bulk phase formation but potential implications for coloration or specific structural roles (Ezra et al., 2024).

A systematic trend was observed regarding the variation in elemental concentration with increased ZnO content. Specifically, as the ZnO proportion in the precursor glasses was elevated, a corresponding reduction was detected in the relative percentages of other major oxides, notably SiO_2, CaO, and Na_2O. This inverse relationship reflects the compositional adjustments made to accommodate higher ZnO loading within the soda lime silica (SLS) glass network (Kaiser and Shugar, 2012). From a structural perspective, the incorporation of ZnO alters the network connectivity by introducing non-bridging

oxygens (NBOs), which act to depolymerize the silicate framework. This substitution not only affects the glass structure but also modulates critical physical attributes such as thermal expansion, refractive index, and elasticity.

The reduction in CaO and Na_2O, in particular, has been strategically optimized to enhance specific material properties. According to Wang and Hon, 1992, decreasing CaO content contributes to improved chemical durability and mechanical resilience, while reductions in alkali oxides like Na_2O suppress excessive ionic mobility, enhancing thermal and structural stability. The balance between network formers (SiO_2) and modifiers (ZnO, Na_2O, CaO) is therefore essential in tailoring the performance characteristics of the glass-ceramic material for targeted applications such as optoelectronics and structural components. These compositional refinements underscore the importance of precise chemical control in the fabrication of advanced glass-ceramic systems.

Table 2: Chemical Composition of ZnO-SLS Glass System (wt.%)

Glass sample/ Oxide	SLS	10ZnO 90SLS	20ZnO 80SLS	30ZnO 70SLS	40ZnO 60SLS	50ZnO 50SLS
SiO_2	69.5±0.1	62.6±0.1	55.6±0.1	48.7±0.1	41.7±0.1	34.9±0.1
Na_2O	12.5±0.1	11.3±0.1	10.0±0.1	8.8±0.1	7.5±0.1	6.3±0.1
CaO	11.3±0.1	10.2±0.1	9.1±0.1	7.9±0.1	6.8±0.1	5.7±0.1
Al_2O_3	2.8±0.1	2.4±0.1	2.2±0.1	1.9±0.1	1.6±0.1	1.3±0.1
MgO	2.0±0.1	1.9±0.1	1.7±0.1	1.5±0.1	1.3±0.1	1.0±0.1
K_2O	1.5±0.1	1.3±0.1	1.2±0.1	1.1±0.1	0.9±0.1	0.7±0.1
ZnO	-	10.0±0.1	19.9±0.1	29.8±0.1	39.9±0.1	49.8±0.1
Others	0.4±0.1	0.3±0.1	0.3±0.1	0.3±0.1	0.3±0.1	0.3±0.1
Total	**100**	**100**	**100**	**100**	**100**	**100**

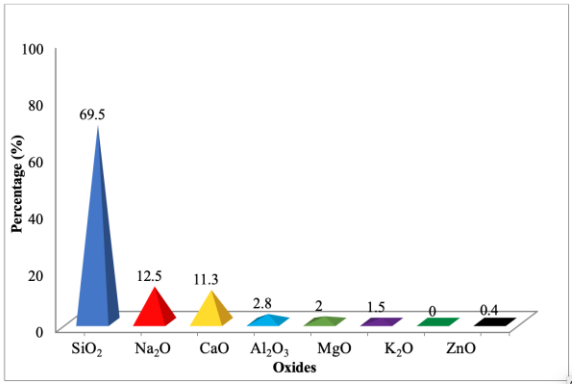

Figure 2: Chemical composition of SLS glass sample

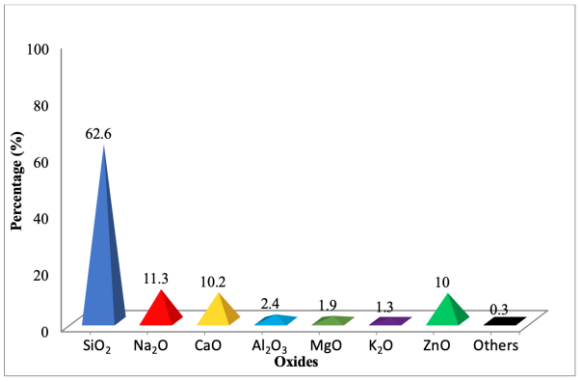

Figure 3: Chemical composition of 10ZnO90SLS glass sample

BJET, 2025, Vol. 20 (2), 5-14

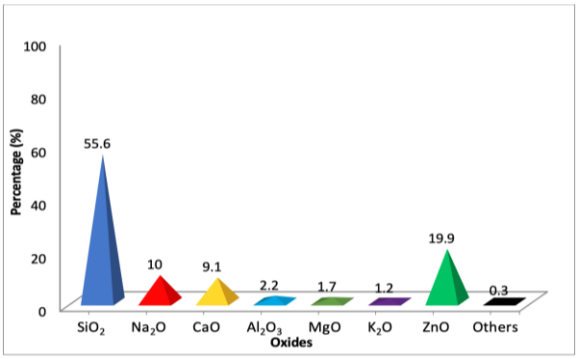

Figure 1: Chemical composition of 20ZnO80SLS glass sample

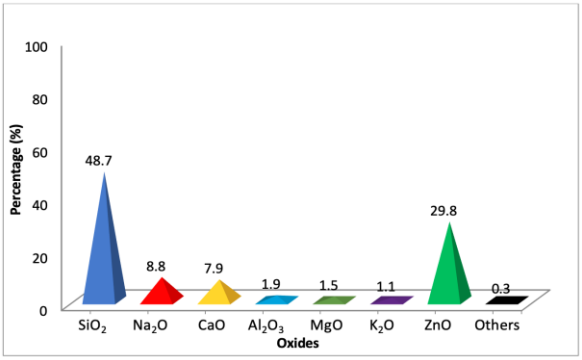

Figure 5: Chemical composition of 30ZnO70SLS glass sample

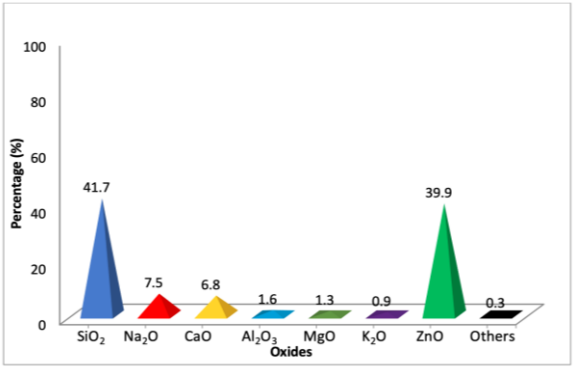

Figure 6: Chemical composition of 40ZnO60SLS glass sample

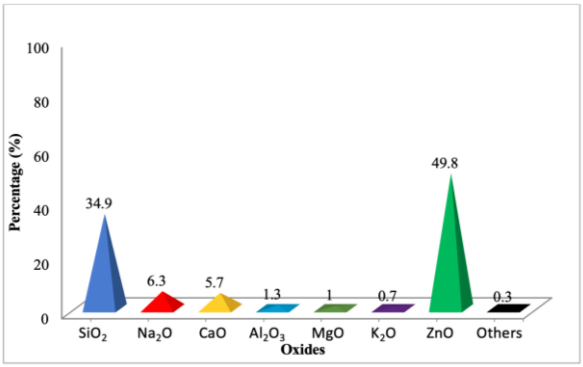

Figure 7: Chemical composition of 50ZnO50SLS glass sample

3.2 DTA Analysis

The effects of the ZnO doping on DTA of all of the glass series at a heating rate of 10 ºC/min are shown in Figure 8. The reduction in melt viscosity with higher ZnO incorporation is a critical factor contributing to the observed decrease in Tg and Tc by approximately 50–60 °C. Zn^{2+} ions, when introduced into the glass structure, disrupt the continuous Si–O–Si network and promote the formation of Zn–O–Si and Zn–O–Zn linkages. These interactions are typically weaker and more flexible than Si–O–Si bridges, resulting in an overall softening of the glass matrix. Consequently, the energy required for viscous flow and nucleation is diminished, making the glass more susceptible to phase transitions at lower temperatures. This behavior is consistent with previous reports in the literature (Zaid et al., 2017), where the addition of intermediate oxides like ZnO has been shown to depress thermal transition points due to their role in enhancing network depolymerization and structural mobility (Zaid et al., 2017: Ozawa, 1971; Strnad and Douglas, 1973; Aboud et al., 2005;).

Moreover, the reduction in Tg and Tc associated with increased ZnO content has significant implications for the glass-ceramic processing window. A lower Tg facilitates easier forming and shaping at reduced energy input, while a lower Tc enhances the potential for controlled nucleation and growth of crystalline phases such as willemite (Zn_2SiO_4) during subsequent heat treatments (Zaid et al., 2017). These changes improve the glass-ceramic's processability and reduce thermal energy demands during sintering. However, care must be taken to maintain a sufficient thermal separation between Tg and Tc to prevent premature crystallization during forming processes. Thus, tailoring ZnO content not only alters the structural rigidity of the SLS glass network but also provides a strategic pathway to engineer the thermal and mechanical performance of glass-ceramic materials (Zaid et al., 2017).

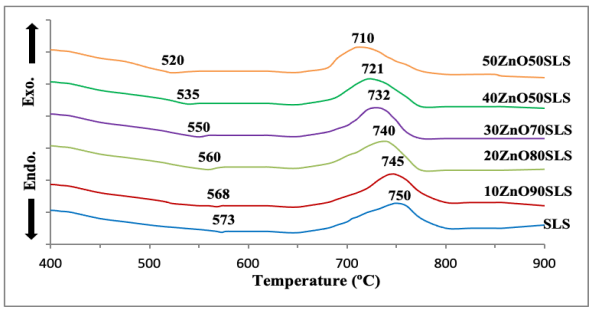

Figure 2: DTA curves of precursor ZnO-SLS glass system

3.3 Density Analysis

Density measurement serves as a vital diagnostic tool for probing structural evolution within oxide glass systems. The correlation between glass composition and structural compactness is commonly investigated through bulk density assessments (Samsudin et al. 2015). In this study, the density of the ZnO–SLS glass samples was determined using the Archimedes method, offering insight into molecular packing efficiency, coordination number variations, and cross-link density within the glass network (Learning, 2021;Zaid et al., 2016). As presented in Figure 9, the density of the samples increased systematically from 2.520 to 2.842 g/cm³ with rising ZnO content. This trend is primarily attributed to the substitution of lighter oxides such as SiO_2, CaO, and Na_2O with heavier ZnO. The atomic mass of Zn (65.390 amu) significantly exceeds those of Si (28.086 amu), Ca (40.078 amu), and Na (22.989 amu), thereby contributing to the overall densification of the glass matrix (Mohd Shofri et al., 2020). Additionally, structural reconfiguration driven by ZnO incorporation likely contributes to this observed density increment (Zaid et al., 2017).

The dual role of ZnO in glass systems—as both a network former and a network modifier—has substantial implications for structural integrity and property tailoring. When incorporated as a network former, Zn^{2+} ions participate in tetrahedral ZnO_4 units, enhancing the glass network by forming covalent Zn–O–Si or Zn–O–Zn linkages. Conversely, ZnO can act as a network modifier, disrupting the Si–O–Si bridges and introducing non-bridging oxygen (NBO) species and associated defects such as dangling bonds. The formation of NBOs reduces network connectivity and mechanical rigidity, thus modifying the structural topology of the glass. Recent studies have shown that Zn^{2+} ions tend to occupy interstitial positions within the open network of SLS glass, promoting the depolymerization of the silicate framework. This effect is characterized by the cleavage of Si–O–Si bonds and the generation of NBOs, leading to a less cross-linked and more structurally relaxed network. Consequently, the increase in ZnO content simultaneously enhances the glass density and modifies its short-range order, illustrating the complex interplay between compositional design and structural response in glass materials (Zaid et al., 2017).

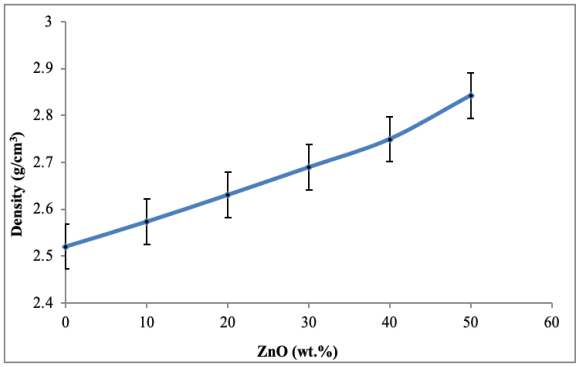

Figure 3: *The average density of ZnO-SLS glass system.*

3.4 XRD Analysis

The X-ray diffraction (XRD) patterns of all glass samples are presented in Figure 10. Each sample exhibits a broad halo within the 2θ range of approximately 20° to 40°, indicative of an amorphous structure. The absence of sharp, continuous, or discrete peaks in the patterns confirms the lack of long-range crystalline order and highlights the predominantly amorphous nature of the glass matrix (Mihailova et al., 2024).

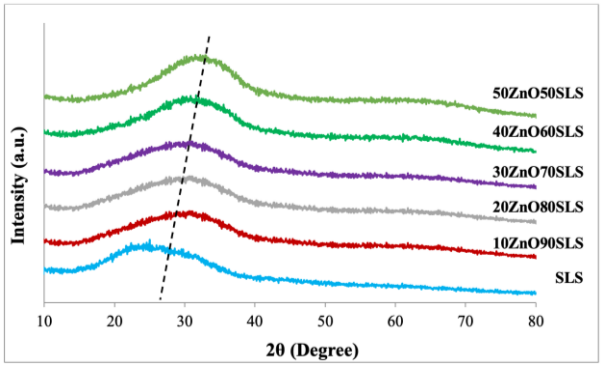

Figure 4: *X-ray diffraction pattern of ZnO-SLS glass system.*

As shown in Figure 10, the position of the broad halo shifts from a lower diffraction angle (~27°) to a higher angle (~33°) with increasing ZnO content, accompanied by a reduction in peak broadening. This narrowing of the amorphous halo suggests a decrease in the average interatomic spacing, corresponding to a reduction in the lattice constant as ZnO concentration increases in the SLS glass matrix (Suzuki et al., 2005). This behavior is likely due to the partial substitution of larger Na^+ (~102 pm) and Ca^{2+} (~100 pm) ions with smaller Zn^{2+} ions (~72 pm) in the glass network. Additionally, the shift in the broad peak towards

angles characteristic of ZnO further supports this substitution effect (Molla et al., 2011).

3.5 FESEM Analysis

Figure 11 presents the phase morphology of the ZnO-SLS-based glass system. As observed in the FESEM micrographs, the surfaces of the precursor glass samples exhibit smooth, featureless textures with no evidence of surface crystallization. This morphological characteristic is indicative of a glassy or amorphous phase (Bateni et al., 2014; Molla et al., 2011). The absence of crystalline features supports the XRD findings, which also confirmed the amorphous nature of the glass samples through the presence of broad diffraction halos and the absence of sharp peak

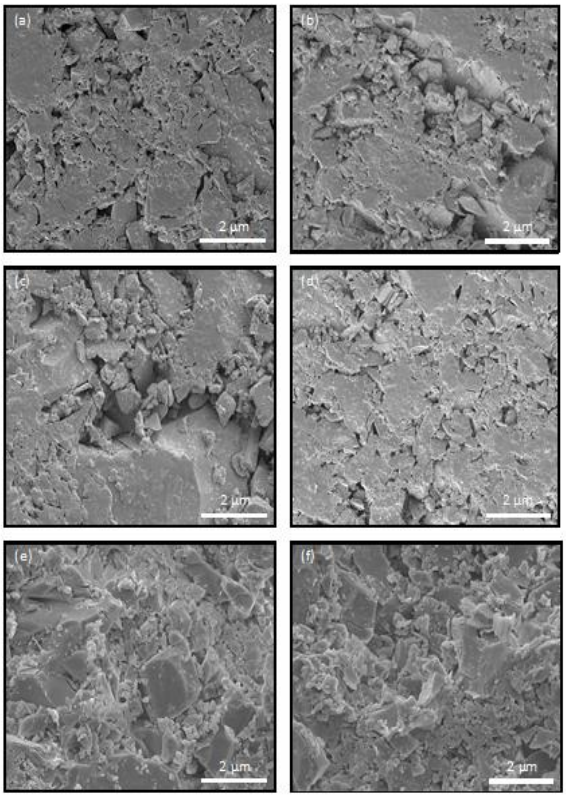

Figure 5: *FESEM images of the ZnO-SLS glass precursor system: (a) pure SLS, (b) 10ZnO–90SLS, (c) 20ZnO–80SLS, (d) 30ZnO–70SLS, (e) 40ZnO–60SLS, and (f) 50ZnO–50SLS.*

Moreover, no significant microstructural differences are observed among the samples, despite the varying ZnO content. This suggests that the incorporation of ZnO up to the tested concentrations does not induce surface crystallization or alter the overall amorphous matrix at the microscopic level. The uniformity in morphology across all compositions implies that ZnO acts as a network modifier or intermediate without disrupting the glass-forming ability of the SLS-based matrix under the current processing conditions (Bateni et al., 2014).

4 Conclusion

This study has successfully demonstrated the synthesis and characterization of a ZnO-doped soda lime silica (SLS) glass system derived from post-consumer waste glass using a conventional melt-quenching technique. The incorporation of ZnO into the glass matrix significantly altered the compositional, thermal, and physical properties of the resulting material, establishing its viability for advanced applications, particularly in optoelectronics. Compositional analysis via EDXRF confirmed that the glass matrix predominantly comprised ZnO, SiO_2, CaO, and Na_2O, with minor and trace oxides contributing to the glass structure and stability. Increasing ZnO content was correlated with a systematic reduction in the concentrations of SiO_2, CaO, and Na_2O, resulting in a glass system optimized for enhanced chemical durability and reduced ionic mobility. This substitution was found to introduce non-bridging oxygen species, thereby depolymerizing the silicate network and modifying key structural characteristics. Differential Thermal Analysis (DTA) revealed a notable decrease in glass transition (Tg) and crystallization temperatures (Tc) with increasing ZnO, attributed to reduced melt viscosity and increased structural flexibility. This thermal behavior not only facilitates energy-efficient processing but also broadens the glass-ceramic processing window by allowing precise control over crystallization dynamics. Furthermore, density measurements showed a consistent increase in bulk density from 2.520 to 2.842 g/cm³, reflecting the replacement of lighter oxides with heavier ZnO and the resultant enhancement in molecular packing and short-range order. The X-ray diffraction patterns of the glass samples exhibited broad halos within the 2θ range of 20° to 40°, confirming their amorphous structure due to the absence of sharp crystalline peaks. A shift in the halo position toward higher angles with increasing ZnO content, along with peak narrowing, suggests reduced interatomic spacing from the substitution of larger Na^+ and Ca^{2+} ions by smaller Zn^{2+} ions. Complementary FESEM analysis revealed smooth, featureless surfaces with no signs of crystallization, indicating that ZnO incorporation does not disrupt the glassy matrix or induce microstructural changes within the examined concentration range.These findings highlight the dual role of ZnO as both a network modifier and former, critically influencing the glass network topology. Overall, the ZnO/SLS glass system presented in this work exemplifies an effective pathway for the valorization of waste glass

into functional materials with tunable properties. The ability to engineer glass properties through ZnO doping paves the way for sustainable and low-energy material solutions, reinforcing the role of recycled materials in the development of next-generation glass-ceramic technologies.

Conflict of Interests

The authors hereby declare and confirm that there are no competing interests associated with the publication of this paper.

Acknowledgments

The researchers gratefully acknowledge the financial support provided by the Malaysian Ministry of Higher Education (MOHE) and Universiti Putra Malaysia through the Fundamental Research Grant Scheme (FRGS) and the Inisiatif Putra Berkumpulan (IPB) research grant. Sincere appreciation also goes to Associate Professor Khamirul Amin Matori from the Department of Physics, Faculty of Science, Universiti Putra Malaysia, for supplying the laboratory tools and equipment used in this study.

References

Abbasi, M., & Hashemi, B. (2014). Fabrication and characterization of bioactive glass-ceramic using soda–lime–silica waste glass. *Materials Science and Engineering: C*, *37*, 399–404.

Abdel-Hameed, S. A. M., Mahani, R., Hamzawy, E. M. A., Almasarawi, Ola. N., & Margha, Fatma. H. (2024). Structural, Physical, Magnetic, and Dielectric Study of Glassy and Crystalline Bismuth Zinc Silicates. *Silicon*, *16*(2),729–740.

Aboud, T. K., Stoch, L., & Środa, M. (2005). Quartz crystallization in soda-lime-silica glass. *Optica Applicata*, *35*(4), 829-836.

Almendro-Candel, M. B., & Jordán Vidal, M. M. (2024). Glasses, Frits and Glass-Ceramics: Processes and Uses in the Context of Circular Economy and Waste Vitrification. *Coatings*, *14*(3), 346.

Baek, C. R., Kim, H. D., & Jang, Y.-C. (2025). Exploring glass recycling: Trends, technologies, and future trajectories. *Environmental Engineering Research*, *30*(3).

Bateni, N. H., Hamidon, M. N., & Matori, K. A. (2014). Effect of soda-lime-silica glass addition on the physical properties of ceramic obtained from white rice husk ash. *Journal of the Ceramic Society of Japan*, *122*(1422), 161–165.

Chima, D. (2023). *Life cycle assessment of flat glass and the implications of thinner and stronger glass*.

Dang, L., Zhang, M., Tian, C., Zhao, S., & Lu, Q. (2017). Solid-state reaction route to synthesis of ordered mesoporous β-Zn2SiO4: Mn-SiO2 composites with ultraviolet and yellow emission. *Optical Materials*, *73*, 241–246.

Del Rio, D. D. F., Sovacool, B. K., Foley, A. M., Griffiths, S., Bazilian, M., Kim, J., & Rooney, D. (2022). Decarbonizing the glass industry: A critical and systematic review of developments, sociotechnical systems and policy options. *Renewable and Sustainable Energy Reviews*, *155*, 111885.

Dyer, T. D. (2014). Glass recycling. In *Handbook of recycling* (pp. 191–209). Elsevier.

Ezra, N. S., Mustafa, I. S., Sayyed, M. I., Dakok, K. K., Fadhirul, I. M., Khazaalah, T. H., Efenji, G. I., Jamil, M., Naeem, H. S., & Oke, A. O. (2024). Synthesis, and impact of GaN deposition on the physical, optical, and structural properties of Nd^{3+}-doped Na_2O borate glasses prepared with soda lime (SLS) glass as a silica source. *Optical Materials*, *155*, 115907.

Ezra, N. S., Mustafa, I. S., Sayyed, M. I., Dakok, K. K., Khazaalah, T. H., Efenji, G. I., Jamil, M., Naeem, H. S., Oke, A. O., & Fadhirul, I. M. (2024a). Review of Recycled Soda-Lime-Silicate (SLS) Glasses for Dosimetric Applications. *Radiation Physics and Chemistry*, 112085.

Francis, A. A., Rawlings, R. D., Sweeney, R., & Boccaccini, A. R. (2004). Crystallization kinetic of glass particles prepared from a mixture of coal ash and soda-lime cullet glass. *Journal of Non-Crystalline Solids*, *333*(2), 187–193.

Franjić, A., & Freestone, I. C. (2018). Glass recycling. *Recikliraj, Ideje Iz Prošlosti [Recycle, Ideas from the Past]. Archaeological Museum in Zagreb, University of Zagreb, and Zagreb Institute of Archaeology, Zagreb*, 145–161.

Imteaz, M. A., Ali, M. Y., & Arulrajah, A. (2012). Possible environmental impacts of recycled glass used as a pavement base material. *Waste Management & Research: The Journal for a Sustainable Circular Economy*, *30*(9), 917–921.

Imteaz, M. A., Arulrajah, A., & Yilmaz, A. G. (2021). Pollutant treatment efficiencies through rainwater tank, recycled foamed glass and geofabrics. *International Journal of Sustainable Engineering*, *14*(5), 963–969.

Ismaeel, A. M., Usman, F., Hayder, G., & Al-Ani, Y. (2023, April). Analysis of mechanical and environmental effects of utilizing waste glass for the creation of sustainable ultra-high performance concrete. *Annales de Chimie: Science des Matériaux, 47*(2).

Kaiser, B., & Shugar, A. (2012). Glass analysis utilizing handheld X-ray fluorescence. *Handheld XRF for Art and Archaeology. Leuven University Press, Leuven*, 449–470.

Kua, H. W., Teoh, W. S., Xu, X., Huang, B., & Geng, Y. (2024). A review of glass recycling policies in Stockholm, Hong Kong SAR and Shanghai from a circular economy perspective. *Journal of Cleaner Production*, *434*, 140068.

Kubanza, N. S. (2025). Analysing the challenges of solid waste management in low-income communities in South Africa: A case study of Alexandra, Johannesburg. *South African Geographical Journal*, *107*(2), 169–189. https://doi.org/10.1080/03736245.2024.2356563

Lakhouit, A., Alhathlaul, N., El Mokhi, C., & Hachimi, H. (2025). Assessing the Environmental Impact of PV Emissions and Sustainability Challenges. *Sustainability (2071-1050)*, *17*(7).

Learning, L. (2021). Archimedes' Principle. *Fundamentals of Heat, Light & Sound*. pp (11-7)

Li, D., Zhou, M., Zhang, Y., Meng, M., Li, X., Lyu, X., Qin, B., Wang, F., & Zhang, Z. (2025). Effects of heat pressing on microstructure and mechanical properties of lithium disilicate glass ceramics with different crystal morphology. *Ceramics International*, *51*(7), 8590–8598.

Liu, G., Huang, Q., Song, K., Pan, Y., & Zhang, H. (2024). Improved method for calculating CO_2 emission from industrial solid wastes combustion system based on fossil and biogenic carbon fraction. *Waste Management*, *174*, 164–173.

Madival, H., & Rajiv, A. (2025). A Comprehensive Review of Bioactive Glasses: Synthesis, Characterization, and Applications in Regenerative Medicine. *Biomedical Materials & Devices*.

Mihailova, I., Harizanova, R., Shtapleva-Dimova, N., Georgiev, H., & Nedkova-Shtipska, M. (2024). Soda Lime Silicate Glasses Containing Iron Oxide-In Vitro Evaluation. *Journal of Chemical Technology and Metallurgy*, *59*(6), 1353–1362.

Mohd Shofri, M. F. S., Mohd Zaid, M. H., Matori, K. A., Fen, Y. W., Yaakob, Y., Jaafar, S. H., Wahab, S. A. A., & Iwamoto, Y. (2020). Phase transformation, optical and emission performance of zinc silicate glass-ceramics phosphor derived from the ZnO–B_2O_3–SLS glass system. *Applied Sciences*, *10*(14), 4940.

Molla, A. R., Tarafder, A., & Karmakar, B. (2011). Synthesis and properties of glasses in the K_2O–SiO_2–Bi_2O_3–TiO_2 system and bismuth titanate ($Bi_4Ti_3O_{12}$) nano glass–ceramics thereof. *Journal of Materials Science*, *46*(9), 2967–2976.

Ozawa, T. (1971). Kinetics of non-isothermal crystallization. *Polymer*, *12*(3), 150–158.

Rashid, S., Sultan, H., Rashid, W., Talpur, B. D., Tulcan, R. X. S., Khan, M. T., Bohnett, E., Korai, M. S., & Zhang, L. (2025). A critical review of opportunities and challenges of solid waste management in an emerging economy-evidence from Pakistan. Environmental Development, 101182.

Samsudin, N. F., Matori, K. A., Liew, J. Y. C., Wing Fen, Y., Zaid, M., Hafiz, M., & Nadakkavil Alassan, Z. (2015). Investigation on Structural and Optical Properties of Willemite Doped Mn_2. *Journal of Spectroscopy*, *2015*.

Singh, A., Tirpude, A., Mathew, N., & Arfin, T. (2025). Gaseous Emissions from Solid Waste Disposal. In *Waste Derived Carbon Nanomaterials. Volume 1* (pp. 95–114). ACS Publications.

Sinton, C. W., & LaCourse, W. C. (2001). Experimental survey of the chemical durability of commercial soda-lime-silicate glasses. *Materials Research Bulletin*, *36*(13–14), 2471–2479.

Strnad, Z., & Douglas, R. W. (1973). Nucleation and crystallization in the soda-lime-silica system. *Phys. Chem. Glasses*, *14*(2), 33–36.

Tulyaganov, D. U., Alves, M. F., Dimitriadis, K., Murtazaev, S., Agathopoulos, S., & Fernandes, H. R. (2025). Fundamentals and advances in production and application of non-stoichiometric lithium disilicate glass-ceramics: A brief review. *Ceramics International, 51*(12), 15067–15076.

Waite, R. (2025). *Rethinking the Concept of Waste and Mass Consumption: Preserving Resources Through Reuse, Repair and Recycling*. Taylor & Francis.

Wang, M. C., & Hon, M. H. (1992). Effect of CaO addition on crystallization processes of Li_2O-Al_2O_3-SiO_2-TiO_2 glasses. *Journal of the Ceramic Society of Japan*, *100*(1167), 1285–1291.

Yao, M., Wang, D., & Zhao, M. (2015). Element Analysis Based on Energy-Dispersive X-Ray Fluorescence. *Advances in Materials Science and Engineering*, *2015*, 1–7.

Zaid, M. H. M., Matori, K. A., Ab, A. S. H., Wahab, Z. A., & Rashid, S. S. A. (2017). Effect of sintering on crystallization and structural properties of soda lime silica glass. *Science of Sintering*, *49*(4), 409–417.

Zaid, M. H. M., Matori, K. A., Ab Aziz, S. H., Kamari, H. M., Wahab, Z. A., Effendy, N., & Alibe, I. M. (2016). Comprehensive study on compositional dependence of optical band gap in zinc soda lime silica glass system for optoelectronic applications. *Journal of Non-Crystalline Solids*, *449*, 107–112.

Zaid, M. H. M., Matori, K. A., Aziz, S. H. A., Kamari, H. M., Wahab, Z. A., Fen, Y. W., & Alibe, I. M. (2016). Synthesis and characterization of low cost willemite based glass–ceramic for opto-electronic applications. *Journal of Materials Science: Materials in Electronics*, *27*(11), 11158–11167.

Zhang, M., Zhai, W., & Chang, J. (2010). Preparation and characterization of a novel willemite bioceramic. *Journal of Materials Science: Materials in Medicine*, *21*(4), 1169–1173.